International Journal on Magnetic Particle Imaging
Vol 6, No 2, Article ID 2004001, 4 Pages

Infinite Science Publishing

Research Article

Exploring Parameters of Magnetic Particles in 1D Field Excitation

Tobias Klemme[a] · Thorsten M. Buzug[a] · Alexander Neumann[a,*]

[a]Institute of Medical Engineering, University of Lübeck, Lübeck, Germany
*Corresponding author, email: {klemme,neumann}@imt.uni-luebeck.de

Received 24 September 2019; Accepted 26 March 2020; Published online 18 April 2020

Abstract

This work explores how different parameters, e.g. magnetic anisotropy and core radius, influence the signal/spectrum of magnetic particles in a one-dimensional excitation field. Simulations are performed using a model considering both the mechanical and magnetization dynamics of the particle. The performed simulations show an increase of amplitude at higher harmonics for anisotropy constants within a certain range. This increase is also observed for different magnetic radii. The obtained knowledge can help to improve the performance of magnetic particles in magnetic particle imaging.

I. Introduction

The properties of magnetic particles have a great influence on different applications such as magnetic particle imaging (MPI) [1] or magnetic particle hyperthermia [2]. Especially in the field of MPI the magnetic response of the particles is often described using Langevin's theory of paramagnetism, where the magnetization only depends on the ratio of magnetic to thermal energy. In reality, many other properties of the nanoparticle and the surroundings have to be taken into account [3–5]. To give an example: the fact that magnetic particles usually exhibit a magnetic anisotropy leads to a non-reversible behavior (hysteresis). According to Langevin's theory of paramagnetism a bigger core diameter results in a steeper magnetization curve (the modulus of the particle magnetic moment is given by $|m_p| = M_S V_C$ where V_C is the volume of the magnetic core and the saturation magnetization M_S is assumed to be constant). However, increasing the core diameter also increases the anisotropy energy $E_A = K V_C$ (assuming uniaxial anisotropy with an anisotropy constant K), which increases the coercive field and remanent magnetization.

As such it is important to study the influence of particle parameters and their influence on the signal in the context of MPI using a proper model to describe the magnetization dynamics and motion of the particle within arbitrary fields. Therefore, models and solving methods to describe the behavior of magnetic nanoparticles in magnetic fields are required and have been introduced by various previous works [3, 6–8].

In order to obtain more insight into the influence of particle parameters on the magnetic particles signal/spectrum, the particle behavior in a 1D excitation field has been simulated for different parameters. This work will focus on the influence of different anisotropy energies on the induced signal $\frac{\mathrm{d}m}{\mathrm{d}t}$ and its corresponding spectrum.

Additionally, it is studied how the core size and magnetic anisotropy affect the harmonics in interdependence. Finally, the scalability of the anisotropy energy is viewed.

10.18416/ijmpi.2020.2004001

II. Material and Methods

II.I. Simulation

The used simulation is introduced by A. Neumann et al. [6]. It describes the dynamics of the particle magnetic moment as well as its mechanical (Brownian) rotation, which are coupled via the magnetic anisotropy. The calculations within the simulation are performed in spherical/Euler coordinates to represent the state of the particle. In order to consider both, Néel and Brownian relaxation of the magnetic moment, coupled equations of motion are necessary. This coupling is achieved by combining the Landau-Lifschitz-Gilbert equation [9] with adapted Euler equations describing the rotational dynamics within fluids [6, 9, 10]. Combining these equation leads to following angular velocities [6]

$$\vec{\omega}_n = \frac{1}{6\eta V_H}\left(\vec{m}\times\vec{H}_{\text{eff}} + \vec{\tau}_{\text{eff}}\right) \tag{1}$$

and

$$\vec{\omega}_m = -\frac{\gamma}{1+\alpha^2}\vec{H}_{\text{eff}} + \left(\frac{|\gamma|\alpha}{1+\alpha^2}\left(\vec{m}\times\vec{H}_{\text{eff}}\right) + \frac{1}{6\eta V_H}\left(M_S V_M\left(\vec{m}\times\vec{H}_{\text{eff}}\right) + \vec{\tau}_{\text{eff}}\right)\right), \tag{2}$$

where $\vec{\omega}_n$ ($\vec{\omega}_m$) is the angular velocity of the particle (magnetic moment), $\vec{n}$ ($\vec{m}$) is the orientation of the particle (magnetic moment), the gyromagnetic ratio γ, the damping constant α, and the hydrodynamic (magnetic) volume V_H (V_M), respectively. The effective magnetic field and torque are given by $\vec{H}_{\text{eff}} = \frac{1}{M_S V_M}\frac{\partial U}{\partial \vec{m}} + \vec{H}_{\text{noise}}$ and $\vec{\tau}_{\text{eff}} = -\frac{\delta U}{\delta \vec{\phi}} + \vec{\tau}_{\text{noise}}$ with the additional (white)-noise terms $\langle H_{\text{noise},i}(t)\, H_{\text{noise},j}(t')\rangle = 2\frac{k_B T\alpha}{\mu_0|\vec{m}|\gamma}\delta_{i,j}\delta(t-t')$ and $\langle F_{\text{noise},i}(t)\, F_{\text{noise},j}(t')\rangle = 12\eta V_H k_B T\delta_{i,j}\delta(t-t')$ to include thermal fluctuations.

Assuming that the magnetic particles are single-domain particles and exhibit uniaxial anisotropy the energy is given by $U = -\vec{m}\cdot\vec{H} + K V_M(\vec{e}\cdot\vec{n})^2$ (Stoner-Wohlfarth-model [11]) where $\vec{e} = \vec{m}/M_S V_M$ is the normalized magnetic moment.

The corresponding Langevin equations in spherical /Euler coordinates can be written as:

$$\frac{\partial\vec{\Phi}_n}{\partial t} = E_{313}\left(\vec{\Phi}_n\right)\cdot\vec{\omega}_n \tag{3}$$

$$\frac{\partial\vec{\Phi}_m}{\partial t} = E_{\text{Sphere}}\left(\vec{\Phi}_m\right)\cdot\vec{\omega}_m \tag{4}$$

with projection matrices E_{313}, E_{Sphere} and Euler angles $\vec{\Phi}_n = (\phi_n, \theta_n, \psi_n)$ and spherical coordinates $\vec{\Phi}_m = (\theta_m, \phi_m)$. Equations (3) and (4) are coupled stochastic differential equations which are solved using the Euler-Maruyama scheme [12].

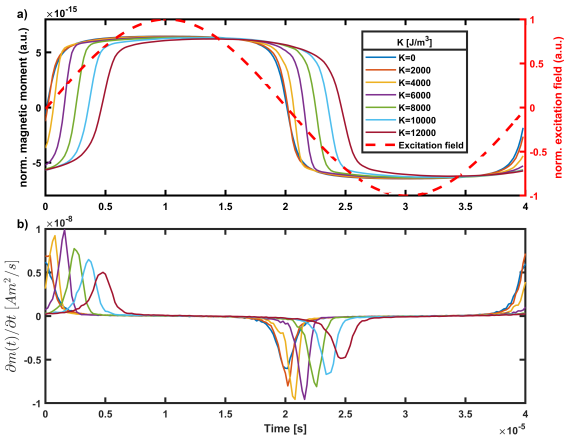

Figure 1: a) Plot of the normalized magnetic moment and the associated excitation signal. An increasing anisotropy energy leads to a larger phase-difference; b) $\frac{dm}{dt}$ for different anisotropy constants. In addition to the phase difference, different anisotropy energies lead to different signal amplitudes.

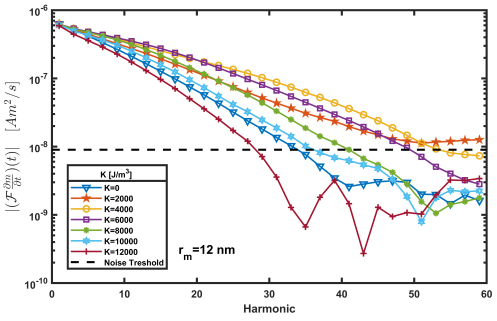

Figure 2: Magnitude of the harmonics in the spectrum of $\frac{dm}{dt}$ for different anisotropy constants. The highest harmonics occur at $K = 4\,\text{kJ/m}^3$. The noise threshold depends on the number of simulated particles and periods.

II.II. Parameters

Within the simulations the particles saturation magnetization M_S is set to 477 464 A/m, and an excitation field strength of 20 mT with a frequency of 25 kHz is chosen. The viscosity of water (1 mPa s) and room temperature (295 K) are used.

This leads to a Brown relaxation time of $\tau_B \approx 0.4821\,\mu\text{s}$ and Néel relaxation times in the range of $\tau_n \approx 24.35\,\text{ns} - 0.42\,\text{s}$ for a K in the range of 0 - 12 kJ/m^2 based on Equations (5) & (6) from [3].

The simulation time step is set to 5 ps whereby the actual output is oversampled to a time step of 0.2 µs. In all simulations the hydrodynamic diameter is set to 50 nm whereas in simulations, where only the anisotropy has been varied, the magnetic core diameter is set to 24 nm. Each simulation has been performed over 6 periods (240 µs) of the excitation frequency with an ensemble of 2000 particles. The run time is in the order of 20 min-

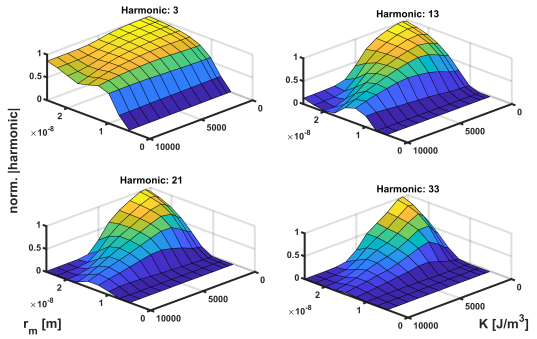

Figure 3: Normalized harmonics (3, 13, 21, 33) for varying magnetic radii and anisotropy constants.

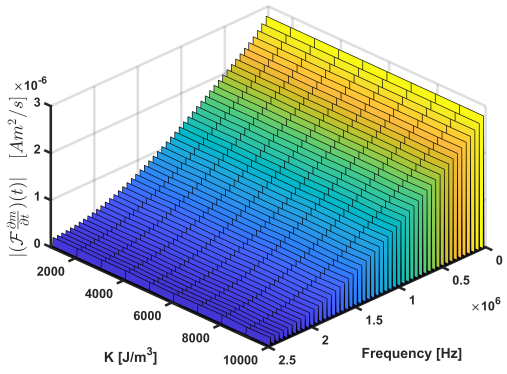

Figure 4: Amplitude spectra for $K = 1-10\,\mathrm{kJ}$ with constant anisotropic energy barrier KV_M and magnetic moment $M_S V_M$.

utes using 4x Intel E5-4657L v2 CPUs. In the following studies, the first period of the simulation is neglected to avoid initialization artifacts, i.e. transient non-periodic behavior, when the magnetic field is applied for the first time, since the magnetic particles are initialized with a random starting orientation and magnetization direction.

III. Results

III.I. Influence of different anisotropy constants

Figure 1a) shows the normalized magnetic moment for different anisotropy constants and the corresponding normalized excitation signal.

The relationship between the time offset and the anisotropy energy is easily recognized and caused by the magnetic anisotropy which exerts an additional torque on the particle's magnetic moment which must be overcome to reverse $\vec{m}$ with respect to the easy axis $\vec{n}$. Thus, a larger magnetic field $\vec{H}$ is necessary to reverse the magnetic moment in the direction of the applied field.

Figure 1b) shows the time derivative of the magnetic moment. It is recognizable that the anisotropy does not only affect the phase between the excitation signal and the magnetic moment, but also influences the magnitude of $\frac{\mathrm{d}m}{\mathrm{d}t}$ and therefore the switching behavior of the particles magnetic moment with respect to the applied field.

For a system-matrix based reconstruction it is important that the measured spectrum contains many and high harmonics [1]. To demonstrate how different anisotropy constants influence the spectrum of the acquired signal $\frac{\mathrm{d}m}{\mathrm{d}t}$, the magnitude of the harmonics is plotted in Figure 2.

It can be observed that the harmonics are larger for certain magnetic anisotropy energies KV_C. In the case of the different anisotropy constants shown in Figure 2 and the used other simulation parameters the highest harmonics occur at an anisotropy constant of $K = 4\,\mathrm{kJ/m^3}$. Both, higher and lower anisotropy constants result in lower harmonics. The case $K = 0$ is identical to the behavior obtainable from the Langevin function.

III.II. Interdependence of anisotropy and magnetic radii

To visualize how harmonics are influenced by different core sizes with different anisotropies, Figure 3 shows a surface plot of different harmonics for different core radii and anisotropy constants. The core radius is varied from 5 nm to 25 nm in 2.5 nm steps. K is varied from 1 to 10 $\mathrm{kJ/m^3}$ in 1 $\mathrm{kJ/m^3}$ steps. Additionally, simulations with 500 and 100 $\mathrm{J/m^3}$ are performed. The overall magnetic moments of the different core sizes are normalized $\tilde{m}(t) = m(t)/NM_S V_C$, where N is the number of particles.

Additionally, the harmonics of every surface plot are normalized to the largest occurring harmonic within the surface. It can be observed that the optimal anisotropy constant decreases with increasing core radius. Yet even for very big core radii a small anisotropy ($K \leq 1000\,\mathrm{J/m^3}$) leads to slightly higher harmonics, particularly at higher frequencies, whereas the harmonics of particles with large magnetic radii and high anisotropy decreases fast. This fast decrease can be explained with an increased Brownian rotation and the resulting friction losses, since Brownian rotation is energetically favorable due to the high anisotropy energy for bigger cores.

III.III. Simulations with constant anisotropy energy barrier and magnetic moment

Due to the fact that the anisotropy energy $E_A = KV_M$ is scalable with the magnetic core size/anisotropy constant

it can be expected, that magnetic particles with identical anisotropic energy and magnetic moment ($M_S V_M$) show equal behavior as long as both $K V_M$ & $M_S V_M$ are kept constant.

Figure 4 shows the amplitude spectra of particles with varied anisotropy constants (1-10 kJ), constant magnetic moment and anisotropy energy.

Where $K V_M = 3 \cdot 10^{-20}$ J and $M_S V_M = 1.44 \cdot 10^{-17}$ Am^2. It is clearly visible that the amplitude spectra are identical as explained above.

IV. Discussion

It has been shown how different anisotropy constants with a fixed magnetic radius or varying magnetic radii and therefore different anisotropy energies can influence the behavior of magnetic particles with a uniaxial anisotropy in a 1D excitation field when Néel and Brownian rotation are considered. At a specific anisotropy, higher harmonics are observed which helps in MPI image reconstruction. The effect of increased amplitudes in higher harmonics caused by uniaxial anisotropies is studied in [4], where Brownian relaxation is not considered and a parallel alignment of the easy axis and the magnetic field is assumed. The results in Figure 2 show that an anisotropy caused increase of harmonic frequency amplitudes can also be observed when Brownian relaxation/rotation is considered. Assuming that the switching behavior of the magnetic moment in a particle can be approximated by the switching behavior of a 2-state system (due to the uniaxial anisotropy) [4], it becomes clear that the increase is particularly dependent on the hydrodynamic radius of the particle and the viscosity of the fluid. This is because the 2-state approximation is only valid if the particle easy axis aligns roughly parallel to the applied field. Therefore, increased amplitudes of harmonic frequencies can only be expected if the particles easy axis' are able to approximately align parallel to the applied field and keep this alignment in average and with respect to the excitation frequency. The particle alignment particularly depends on the hydrodynamic radius and the viscosity of the surrounding fluid.

It must be considered that the simulations have been performed with a 1D sinusoidal excitation field. For other frequencies or 2D/3D excitation the dynamics of a magnetic particle and its magnetic moment are different and thus other values of particle properties will be advantageous or disadvantageous. Nevertheless, it is shown that well-chosen particle parameters will improve MPI performance.

V. Conclusions

Using a varying anisotropy constant and in the second case additionally varying magnetic radii, it is exemplified how particle properties influence the signal harmonics relevant for MPI. Additionally, it is shown that the scalability of the anisotropy energy leads to the expected equal behavior. Several simulations can be done to gain knowledge how properties like excitation frequency, multi-dimensional excitation, hydrodynamic radius, viscosity, particle distribution or as described, the magnetic anisotropy change the acquired signal. This knowledge helps to synthesize performing magnetic particles for application in MPI or magnetic particle hyperthermia.

Acknowledgments

This work was funded by the German Federal Ministry of Education and Research, contract number 13GW0069B.

References

[1] B. Gleich and J. Weizenecker. Tomographic imaging using the nonlinear response of magnetic particles. *Nature*, 435(7046):1214–1217, 2005, doi:10.1038/nature03808.

[2] S. Dutz and R. Hergt. Magnetic particle hyperthermia—a promising tumour therapy? *Nanotechnology*, 25(45):452001, 2014, doi:10.1088/0957-4484/25/45/452001.

[3] D. B. Reeves and J. B. Weaver. Combined Néel and Brown rotational Langevin dynamics in magnetic particle imaging, sensing, and therapy. *Applied Physics Letters*, 107(22):223106, 2015, doi:10.1063/1.4936930.

[4] J. Weizenecker, B. Gleich, J. Rahmer, and J. Borgert. Micromagnetic simulation study on the magnetic particle imaging performance of anisotropic mono-domain particles. *Physics in Medicine and Biology*, 57(22):7317–7327, 2012, doi:10.1088/0031-9155/57/22/7317.

[5] S. Biederer, T. F. Sattel, T. Knopp, K. Lüdtke-Buzug, B. Gleich, J. Weizenecker, J. Borgert, and T. M. Buzug, The influence of the particlesize distribution on the image resolution in magnetic particle imaging, in *ESMRMB Congress 2009*, 499, 2009.

[6] A. Neumann and T. M. Buzug, Stochastic simulations of magnetic particles: Comparison of different methods, in *International Workshop on Magnetic Particle Imaging*, 213, 2018.

[7] J. Weizenecker, B. Gleich, J. Rahmer, and J. Borgert, Particle dynamics of mono-domain particles in magnetic particle imaging, in *Magnetic Nanoparticles*, 3–15, WORLD SCIENTIFIC, 2010. doi:10.1142/9789814324687_0001.

[8] C. Shasha, E. Teeman, and K. M. Krishnan. Harmonic Simulation Study of Simultaneous Nanoparticle Size and Viscosity Differentiation. *IEEE Magnetics Letters*, 8:1–5, 2017, doi:10.1109/LMAG.2017.2754238.

[9] W. T. Coffey and Y. P. Kalmykov, The Langevin Equation, 3rd Ed. World Scientific, 2017,

[10] M. I. Shliomis and V. I. Stepanov, Theory of the Dynamic Susceptibility of Magnetic Fluids, in, 2007, 1–30. doi:10.1002/9780470141465.ch1.

[11] E. Stoner and E. P. Wohlfarth. A mechanism of magnetic hysteresis in heterogeneous alloys. *Philosophical Transactions of the Royal Society of London. Series A, Mathematical and Physical Sciences*, 240(826):599–642, 1948, doi:10.1098/rsta.1948.0007.

[12] P. E. Kloeden and E. Platen, Numerical Solution of Stochastic Differential Equations, 2nd Ed. Springer Berlin Heidelberg, 1995,

